



Boundary mode lubrication of articular cartilage with a biomimetic diblock copolymer

Zhexun Sun^a, Elizabeth Feeney^a, Ya Guan^b, Sierra G. Cook^b, Delphine Gourdon^{b,c}, Lawrence J. Bonassar^{a,d}, and David Putnam^{a,e,1}

^aMeinig School of Biomedical Engineering, Cornell University, Ithaca, NY 14853; ^bDepartment of Materials Science and Engineering, Cornell University, Ithaca, NY 14853; ^cDepartment of Physics, University of Ottawa, Ottawa, ON K1N 6N5, Canada; ^dSibley School of Mechanical and Aerospace Engineering, Cornell University, Ithaca, NY 14853; and ^eSmith School of Chemical and Biomolecular Engineering, Cornell University, Ithaca, NY 14853

Edited by Robert Langer, Massachusetts Institute of Technology, Cambridge, MA, and approved May 8, 2019 (received for review January 14, 2019)

We report the design of a diblock copolymer with architecture and function inspired by the lubricating glycoprotein lubricin. This diblock copolymer, synthesized by sequential reversible addition–fragmentation chain-transfer polymerization, consists of a cationic cartilage-binding domain and a brush-lubricating domain. It reduces the coefficient of friction of articular cartilage under boundary mode conditions (0.088 ± 0.039) to a level equivalent to that provided by lubricin (0.093 ± 0.011). Additionally, both the EC_{50} (0.404 mg/mL) and cartilage-binding time constant (7.19 min) of the polymer are comparable to purified human and recombinant lubricin. Like lubricin, the tribological properties of this polymer are dependent on molecular architecture. When the same monomer composition was evaluated either as an AB diblock copolymer or as a random copolymer, the diblock effectively lubricated cartilage under boundary mode conditions whereas the random copolymer did not. Additionally, the individual polymer blocks did not lubricate independently, and lubrication could be competitively inhibited with an excess of binding domain. This diblock copolymer is an example of a synthetic polymer with lubrication properties equal to lubricin under boundary mode conditions, suggesting its potential utility as a therapy for joint pathologies like osteoarthritis.

lubricin | biomimetic | boundary mode lubrication | osteoarthritis

As the primary bearing surface, articular interfaces exhibit remarkable tribological function over decades of use (1). The impressive lubricity and durability of articular cartilage has inspired the design of synthetic macromolecules that mimic the architecture of lubricating biomolecules (2–9). However, very few synthetic polymers achieve lubrication comparable to endogenous articular surfaces, strongly supporting the need for new synthetic materials that rival the efficacy of natural materials. Here, we report the design and synthesis of a diblock copolymer with substantial lubrication capacity whose architecture is inspired by the structure of lubricin, a natural glycoprotein that lubricates joints under boundary mode conditions (i.e., high normal load and slow speed).

Lubricin is a glycosylated protein found in synovial fluid (10) which plays a pivotal role in joint boundary mode lubrication (11, 12) and the prevention of osteoarthritis (11, 13, 14). Lubricin reduces the coefficient of friction (COF) of articular cartilage under boundary mode conditions by as much as 70% (12). The potent lubrication arises from its structure: a central mucin-like domain to attract and retain water and a cartilage-binding domain at the C terminus to affix the molecule to the cartilage surface (15). This architecture of lubricin is crucial to boundary mode lubrication of articular cartilage, as denaturation in either domain of lubricin causes partial or complete loss of lubrication capability (15, 16). We defined the design criteria for a synthetic boundary mode lubricant inspired by lubricin's architecture: a diblock copolymer consisting of a large lubrication block ($M_n \sim 200$ kDa) to mimic the mucin-like domain of lubricin and a small cartilage-binding block ($M_n \sim 3$ kDa) to mimic the C-terminus domain (Fig. 1). The lubrication domain of the diblock copolymer

is made of a polyacrylic acid (pAA) backbone with polyethylene glycol (PEG) brushes, which enables the polymer to retain water and to resist compression. The binding domain is made of a pAA backbone decorated with quaternary ammonia groups to non-specifically interact with negatively charged cartilage surface components such as aggrecan. Applying this polymer to lubricin-deficient bovine articular cartilage in PBS resulted in a significant reduction in COF under boundary mode conditions.

Results and Discussion

The diblock copolymer was synthesized in three steps, as shown in Fig. 2. Starting with RAFT (reversible addition–fragmentation chain-transfer) polymerization of 2-(dimethylamino)ethyl acrylate, a precursor “prebinding” domain was produced (17). Subsequent RAFT polymerization of poly(ethylene glycol) methyl ether acrylate (M_n 480), using the “prebinding” domain as the macroinitiator, added the lubrication domain to the copolymer. Finally, the tertiary amines in the “prebinding” cartilage-binding domain precursor were converted to quaternary by treatment with an excess of ethyl bromide to give the final product [$M_n \sim 200$ kDa, polydispersity index (PDI) = 1.6].

To evaluate the polymer as a synthetic boundary mode lubricant we assessed its tribological characteristics using a custom-built tribometer (18). Cartilage samples were obtained from the patellofemoral groove of neonatal bovine stifles and incubated in

Significance

Lubricin is a glycoprotein that protects cartilage in weight-bearing joints under boundary mode conditions, which defines the conditions under which physical cartilage damage takes place. The natural expression of lubricin decreases with age, and when the joint is damaged. Replacement of lubricin by intraarticular injection reestablishes boundary mode lubrication and can protect against osteoarthritis. However, the manufacture of lubricin is difficult. We set out to create a synthetic mimetic of lubricin by mimicking its structure and functional composition. The result is a diblock copolymer that reduces the coefficient of friction on cartilage, under boundary mode conditions, to a level equivalent to native lubricin. This paper reports coefficients of friction in a boundary mode system that are equivalent to lubricin.

Author contributions: Z.S., E.F., Y.G., S.G.C., D.G., L.J.B., and D.P. designed research; Z.S., E.F., Y.G., and S.G.C. performed research; Z.S., D.G., L.J.B., and D.P. analyzed data; and Z.S., L.J.B., and D.P. wrote the paper.

Conflict of interest statement: Z.S., L.J.B., and D.P. are listed as inventors on a patent filing. The patent is not yet issued and the patent is not licensed to any entity.

This article is a PNAS Direct Submission.

Published under the PNAS license.

¹To whom correspondence may be addressed. Email: dap43@cornell.edu.

This article contains supporting information online at www.pnas.org/lookup/suppl/doi:10.1073/pnas.1900716116/-DCSupplemental.

Published online June 4, 2019.

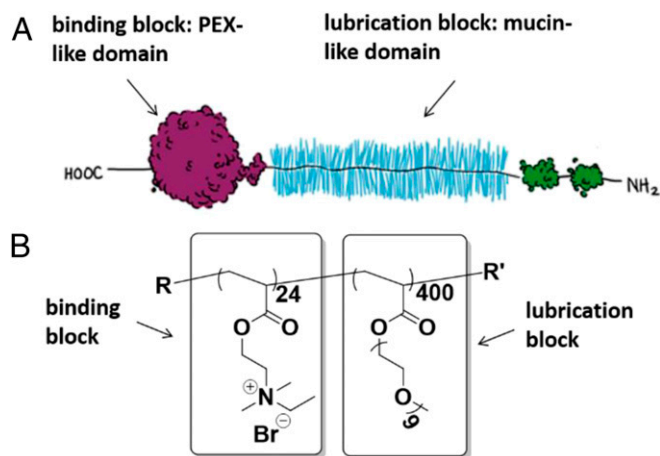


Fig. 1. (A) Schematic representation of lubricin, the native boundary mode lubricant in synovial fluid showing the PEX-like cartilage-binding domain and the mucin-like lubricating domain. (B) The synthetic diblock copolymer mimetic of lubricin showing the molecular compositions that mimic the functional domains of lubricin.

1.5 M NaCl to remove surface-associated synovial fluid contents (19). Samples were incubated in PBS and then in polymer (3 mg/mL in PBS) for 120 min to saturate the cartilage surface. The cartilage samples were loaded onto the tribometer in a PBS bath and evaluated under boundary mode conditions (30% compressive strain and linear oscillation speeds of 0.3 mm/s). Incubating the stripped cartilage with the diblock copolymer solution resulted in a decrease in COF from 0.391 ± 0.020 to 0.088 ± 0.039 ($n = 4-11$, $P < 0.0001$), which is equivalent to lubricin-treated groups (COF = 0.093 ± 0.01112 , shown as the dashed line in Fig. 3). To establish the importance of the diblock architecture on lubrication, the individual cartilage-binding and cartilage-lubricating domains were also evaluated under the same conditions. Neither individual domain decreased COF, supporting the premise that both the binding and lubricating blocks of the copolymer are necessary to lubricate cartilage under boundary mode conditions.

The importance of the binding block to lubrication and its interaction with the cartilage surface was further demonstrated by a competitive binding analysis. The COFs of cartilage samples were measured after exposure to solutions composed of combinations of the binding block and the diblock copolymer in molar ratios ranging from 100:1 to 1:1 ([binding block:diblock copolymer]). The COFs of samples incubated with different molar ratios of [binding block: diblock copolymer] exhibited a dose-response behavior (Fig. 4), wherein higher concentrations of the binding domain inhibited lubrication by the diblock copolymer, suggesting that intimate interaction of the polymers with the cartilage surface is crucial for effective cartilage lubrication.

To further establish the importance of the diblock copolymer architecture on lubrication, a random copolymer with the same monomer composition as the diblock copolymer was synthesized. The failure of this polymer to lubricate articular cartilage under the same tribological conditions (Fig. 5A) emphasized the importance of the diblock copolymer architecture. An accompanying study on the effect of molecular architecture on binding and lubrication was completed using negatively charged mica surfaces in a surface force apparatus (SFA) to show that the lubricity characteristics were consistent between different surface types (20). Mica surfaces that were preincubated with the polymers in solution at 3 mg/mL for 120 min were sheared in PBS under boundary conditions (6-MPa compression load and linear oscillation speed of 30 μ m/s). Similar to the results obtained for cartilage tribology, the measured COFs were 0.493 ± 0.082 for

the random copolymer and 0.122 ± 0.035 for the diblock copolymer (Fig. 5A $n = 3-4$, $*P < 0.0001$). Polymer film thickness on the mica surface was also characterized by measuring normal force as a function of distance between surfaces (Fig. 5B). At the onset of interaction, the diblock copolymer showed an uncompressed film thickness (61.2 ± 2.6 nm) twice as thick as its hydrodynamic size (24.8 ± 0.3 nm), suggesting a double molecular layer coating between the two mica surfaces, whereas the random copolymer exhibited a binary film thickness distribution (36.0 ± 13.5 nm) that matched with either one- or two-molecular-layer thickness (hydrodynamic size: 21.4 ± 1.2 nm), indicating an insufficient coating on both mica surfaces. Under compression, the random copolymer also showed a much smaller thickness (3.6 ± 0.7 nm vs. 10.4 ± 0.6 nm) in comparison with the diblock copolymer, which approaches the distance measured between bare mica surfaces in PBS. These data suggest that while both polymers formed a layer on the mica surface at the beginning of the experiment, the weak electrostatic interaction between the random copolymer and the mica surface failed to maintain the polymer film or to support the normal force throughout the analysis, thereby allowing the polymers to be forced out of the contact zone during compression. The boundary lubrication mode is defined as when the frictional properties are primarily governed by solid–solid interactions (21), and therefore largely dependent on the topology and chemical properties of the opposing surfaces. It is critical for a boundary mode lubricant to form a molecular layer that effectively coats the cartilage surface and that supports the normal load. The individual positively charged quaternary ammonia groups that are randomly distributed in the polymer backbone were not able to efficiently bind to either cartilage or mica surfaces, which again demonstrates the importance of the diblock architecture for lubrication.

To better understand the effectiveness of the diblock copolymer on cartilage lubrication, some key lubrication characteristics were measured and compared with those of natural lubricin. Specifically, a dosing study was performed using cartilage samples that were treated with polymer solutions ranging from 0.01 to 10 mg/mL. The COFs (Fig. 6A) exhibited a dose-response behavior ($R^2 = 0.89$), which at the higher concentrations ($EC_{50} = 0.404$ mg/mL) were effectively reduced to a level comparable to that of naturally lubricated cartilage. Also, the binding kinetics of the diblock copolymer to the cartilage surface was measured in which cartilage samples were incubated at a saturation concentration (1 mg/mL) of polymer over time. When fit to a one-phase decay model ($R^2 = 0.95$), the binding kinetics curve (Fig. 6B) revealed a binding time constant (τ) of 7.19 min, which is comparable to that of natural lubricin (~ 9 min; ref. 12).

Synthetic polymers with structures that mimic natural biolubricants have been extensively studied over the past few decades. Inspired by natural bottle-brush polyelectrolytes, Spencer and coworkers explored a range of mucin analogs featured with a polylysine backbone and grafted PEG (2, 3, 22) or dextran (23) side chains to reduce the COFs on mica surfaces. Israelachvili and coworkers (5) also reported a bioinspired bottle brush polymer that exhibited extremely low friction and Amontons-like behavior characterized by SFA. Both works report effective

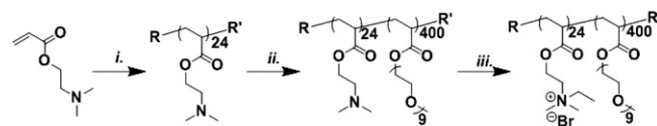


Fig. 2. Synthesis of a lubricin-mimetic diblock copolymer. (i) ACPA, CPADB, anisole, 70 °C. (ii) ACPA, DMAEA, anisole, 65 °C. (iii) EtBr, acetone, room temperature.

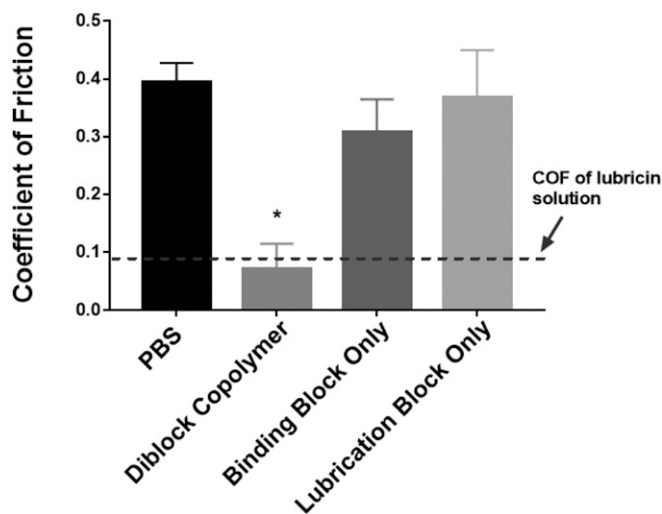


Fig. 3. The lubricin-mimetic diblock copolymer significantly decreases COF of articular cartilage compared with samples treated with PBS, binding block only, or lubrication block only ($*P < 0.0001$). Dashed line represents COF of samples tested in recombinant human lubricin solution at 50 $\mu\text{g}/\text{mL}$ (12). One-way ANOVA was used to determine the statistical difference among the tribological results associated with the polymers in solution and the controls on articular cartilage.

synthetic lubricants using pristine mica surfaces. However, while these materials lubricated the mica surface, the physiological relevance of the results is unknown. Grinstaff and coworkers (7) reported a more physiologically relevant polyanionic biolubricant that performs similar to synovial fluid in an ex vivo human cartilage mode. By mimicking the structure of hyaluronic acid, this polymer reduced the friction at the interface of cartilage and demonstrated its potential in joint lubrication as a new type of viscosupplement. In our previous work, an analog of bottle-brush polymers with a mucin-like structure successfully lubricated articular cartilage under boundary mode condition with COF ranging from 0.140 ± 0.024 to 0.248 ± 0.030 , and binding time constants ranging from 20 to 39 min (24). However, the cartilage binding mechanism(s) that led to these results were unclear and the low binding limited their further application. Elisseff and coworkers (25) cleverly bound cartilage-binding peptides to hyaluronic acid to facilitate its close interaction with tissue surfaces to induce lubrication. Most recently, Benetti and coworkers (26) reported the protection of cartilage from enzymatic degradation through the covalent linkage of cyclic polymer grafts to the cartilage surface.

In this work, where both key lubrication characteristics are engineered into the lubricant by adopting a diblock architecture that facilitates binding and localization of the polymer to the cartilage surface, we show the importance of polymer architecture to lubrication. The diblock copolymer with its lubricin-mimetic structure successfully lubricates articular cartilage surfaces in the boundary mode as effectively and efficiently as natural lubricin. This work demonstrates the importance of the polymer architecture to its tribological properties and the necessity for the coexistence of binding and lubrication blocks for effective lubrication under these conditions. This approach toward the molecular design of boundary mode lubricants could serve as a guide for future synthetic lubricants with even greater efficacy.

Materials and Methods

All chemicals were purchased from Aldrich or Fisher at the highest purity grade. All monomers were purified by a column filled with aluminum oxide (base or neutral) before use. The ^1H NMR spectra were performed on an

Inova 400-MHz spectrometer with deuterated chloroform or deuterium oxide as the solvent. Broad or overlapping peaks, noted in spectra of polymers, are denoted "br." Degree of polymerization was determined by initial monomer to CTA ratio and monomer conversion. Gel permeation chromatography (GPC) was performed with phosphate buffer saline (pH 7.4) at a flow rate of 0.8 mL/min. The eluent flowed through a Waters gel permeation chromatography system equipped with three Waters Ultrahydrogel columns in series (2,000 Å, 500 Å, and 250 Å) at 30 °C. The molecular weights were measured relative to poly(methacrylic acid), sodium salt standards (1,670–110,000 g/mol). DMAEA = 2-(dimethylamino)ethyl acrylate, ACPA = 4,4'-azobis(4-cyanopentanoic acid), CPADB = 4-cyano-4-(phenyl-carbonothioylthio)pentanoic acid, and PEGMEA = poly(ethylene glycol) methyl ether acrylate, $M_n = 480$. $R = -\text{C}(\text{CH}_3)(\text{CN})\text{CH}_2\text{CH}_2\text{COOH}$ and $R' = -\text{S}(\text{C} = \text{S})\text{Ph}$.

Synthesis of PDMAEA₂₄. DMAEA (4.30 g, 30 mmol) was added to a solution containing ACPA (14.0 mg, 0.05 mmol) and CPADB (139.5 mg, 0.5 mmol) in 5 mL of anisole. The mixture was deoxygenated by five freeze–vacuum–thaw cycles before it was heated to 70 °C with stirring for 48 h. The reaction was then quenched by liquid nitrogen freezing, and the polymer gel was precipitated by the addition of 20 mL of hexane and vigorously stirring for 30 min. After decanting the solvent, the residue was redissolved in 5 mL of dichloromethane and precipitated after addition of 20 mL of hexane and vigorously stirring for 30 min (process was repeated four times) to yield a gel (1.68 g, 39% yield); ^1H NMR(400 MHz, CDCl_3): δ 4.13 [br, 2H, $-\text{C}(\text{O})\text{O}-\text{CH}_2-\text{CH}_2-$], 2.55 [br, 2H, $-\text{O}-\text{CH}_2-\text{CH}_2-\text{N}(\text{CH}_3)_2$], 2.31 [br, 7H, $-\text{N}(\text{CH}_3)_2$, $-\text{CH}_2\text{CH}(\text{C} = \text{O})-$], 2.02–1.36 [m, 2H, $-\text{CH}_2\text{CH}(\text{C} = \text{O})-$], 5.30 (s, residue dichloromethane).

Synthesis of PDMAEA₂₄–PEGMEA₄₀₀ (Diblock Copolymer). PEGMEA (3.46 g, 7.2 mmol) was added to a solution containing PDMAEA₂₄ (30.9 mg, 0.009 mmol) and ACPA (0.5 mg, 0.0018 mmol) in 6 mL of anisole. The mixture was deoxygenated by five freeze–vacuum–thaw cycles before it was heated to 65 °C with stirring for 8 h. The reaction was then quenched by liquid nitrogen freezing, and the residue polymer gel was precipitated by addition of 20 mL of hexane and vigorously stirring for 30 min. After decanting the solvent, the residue was redissolved in 5 mL of dichloromethane and precipitated by addition of 20 mL of hexane and vigorously stirring for 30 min (process repeated four times) to yield a gel (1.68 g, 48% yield); ^1H NMR (400 MHz, CDCl_3): δ 4.13 [br, 2H, $-\text{C}(\text{O})\text{O}-\text{CH}_2-\text{CH}_2-$], 3.75–3.44 (m, 34H, $-\text{O}-\text{CH}_2-\text{CH}_2-\text{O}-$), 3.35 (s, 3H, $-\text{O}-\text{CH}_3$), 2.24 [br, \sim 1H, $-\text{CH}_2\text{CH}(\text{C} = \text{O})-$], $-\text{N}(\text{CH}_3)_2$], 1.93–1.26 [m, 2H, $-\text{CH}_2\text{CH}(\text{C} = \text{O})-$], 5.30 (s, residue dichloromethane). The resulting polymer was characterized by GPC using the method described above: $M_n = 44,900$; PDI = 1.58.

Synthesis of qPDMAEA₂₄–PEGMEA₄₀₀ (Diblock Copolymer). Ethyl bromide (0.3 mL, 4.0 mmol) was added dropwise into a solution containing PDMAEA₂₄–PEGMEA₄₀₀ (865.9 mg) in 3 mL of acetone at 0 °C. The mixture was stirred for

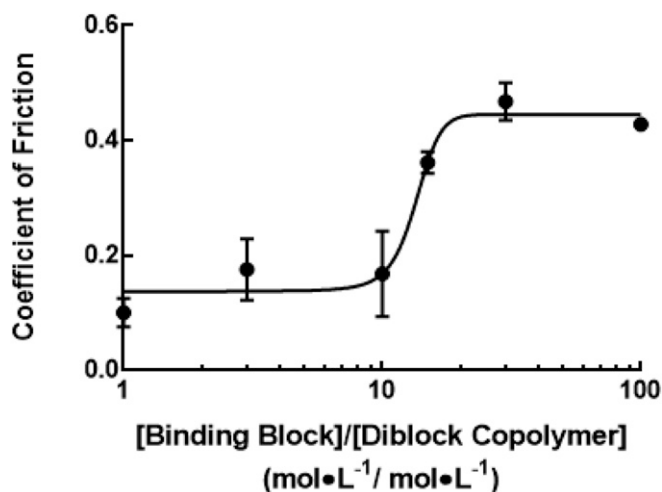


Fig. 4. Competitive inhibition analysis showing the binding block acts as an inhibitor of lubrication when mixed with the diblock copolymer at varying molar ratios. Line is a model fit of a sigmoidal dose–response relationship ($R^2 = 0.87$, $\text{IC}_{50} = 13.45$, $n = 3$ –9, error bars represent ± 1 SD).

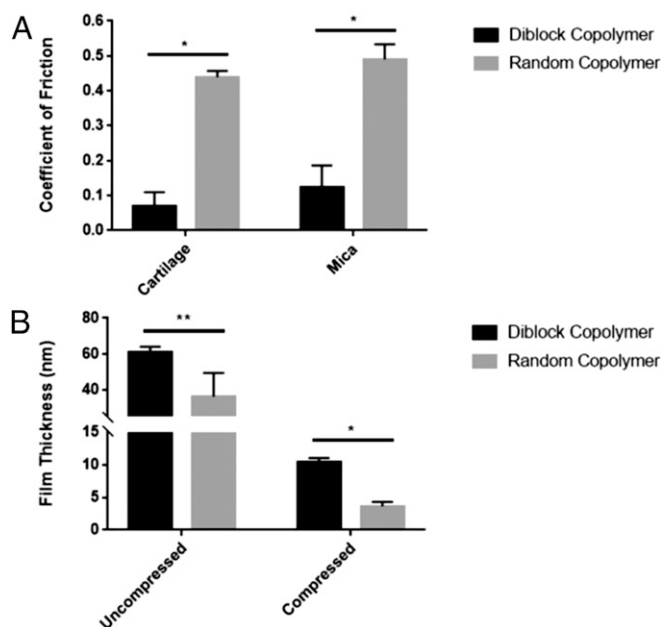


Fig. 5. (A) Random copolymer with the same composition but different architecture failed to lubricate cartilage and mica in comparison with the diblock copolymer architecture ($n = 4-6$, $*P < 0.0001$). (B) Mica samples treated with random copolymer had smaller film thickness under both uncompressed and compressed conditions in comparison with diblock copolymer using SFA measurement ($n = 3-5$, $*P < 0.0001$, $**P < 0.01$), indicating a less efficient binding of random copolymer to the mica surface. Two-way ANOVA was used to determine the statistical difference among the tribological results of the diblock copolymer and the controls on articular cartilage. Student's t test was used to determine the statistical difference of the film thickness of diblock copolymer and random copolymer under uncompressed and compressed conditions individually. Data are presented as mean \pm SD.

48 h at room temperature and was then concentrated by evaporating the solvent with a dry nitrogen flow. The residue was dissolved in 3 mL of dichloromethane and precipitated with addition of 15 mL of hexane and vigorously stirring for 30 min (process repeated five times). The product was then dissolved in deionized (DI) water and further purified by dialysis using Spectra/Por regenerated cellulose dialysis tubing (2 kDa MWCO) against DI water for an additional 48 h before lyophilization. The product (851 mg) was collected as viscous gel in 98% yield; $^1\text{H NMR}$ (400 MHz, D_2O): δ 4.08 [br, 2H, $-(\text{C}=\text{O})\text{O}-\text{CH}_2-\text{CH}_2-$], 3.75–3.46 (m, 34H, $-\text{O}-\text{CH}_2-\text{CH}_2-\text{O}-$), 3.21 (s, 3H, $-\text{O}-\text{CH}_3$), 3.02 [s, $\sim 0.2\text{H}$, $-\text{N}^+(\text{CH}_3)_2\text{CH}_2\text{CH}_3$], 2.21 [br, 1H, $-\text{CH}_2\text{CH}(\text{C}=\text{O})-$], 2.01–1.36 [m, 2H, $-\text{CH}_2\text{CH}(\text{C}=\text{O})-$], 1.25 [br, ~ 0.1 H, $-\text{N}^+(\text{CH}_3)_2\text{CH}_2\text{CH}_3$]. The resulting polymer was characterized with GPC using the method described above: $M_n = 46,100$; $\text{PDI} = 1.58$.

Synthesis of qPDMAEA₂₄ (Binding Block). Ethyl bromide (5 mL, 67 mmol) was added dropwise into a solution containing PDMAEA₂₄ (1.2 g, 0.35 mmol) in 50 mL of acetone at 0 °C. The mixture was stirred for 48 h at room temperature and was then concentrated by evaporating most of the solvent with a dry nitrogen flow. The residue was first purified by dissolution in 20 mL of methanol followed by precipitation through the addition of 100 mL of hexane and vigorously stirring for 30 min (process repeated five times). The purified product was then dissolved in DI water and further purified by dialysis using Spectra/Por regenerated cellulose dialysis tubing (2 kDa MWCO) against DI water for an additional 48 h before lyophilization. The product (1.95 g) was collected as orange crystal in 92% yield; $^1\text{H NMR}$ (400 MHz, D_2O): δ 4.40 [br, 2H, $-(\text{C}=\text{O})\text{O}-\text{CH}_2-\text{CH}_2-$], 3.61 [br, 2H, $-\text{O}-\text{CH}_2-\text{CH}_2-\text{N}^+(\text{CH}_3)_2\text{CH}_2\text{CH}_3$], 3.38 [br, 2H, $-\text{N}^+(\text{CH}_3)_2\text{CH}_2\text{CH}_3$], 3.02 [s, 6H, $-\text{N}^+(\text{CH}_3)_2\text{CH}_2\text{CH}_3$], 2.41 [br, 1H, $-\text{CH}_2\text{CH}(\text{C}=\text{O})-$], 2.02 to 1.45 [m, 2H, $-\text{CH}_2\text{CH}(\text{C}=\text{O})-$], 1.26 [s, 3H, $-\text{N}^+(\text{CH}_3)_2\text{CH}_2\text{CH}_3$].

Synthesis of PEGMEA₄₀₀ (Lubrication Block). PEGMEA (3.46 g, 7.2 mmol) was added to a solution containing CPADB (2.51 mg, 0.009 mmol) and ACPA (0.5 mg, 0.0018 mmol) in 6 mL of anisole. The mixture was deoxygenated by five

freeze–vacuum–thaw cycles before it was heated to 65 °C with stirring for 8 h. The reaction was then quenched by liquid nitrogen freezing, and the polymer gel was precipitated by addition of 20 mL of hexane and vigorously stirring for 30 min. After decanting the solvent, the residue was redissolved in 5 mL of dichloromethane and precipitated by the addition of 20 mL of hexane and vigorously stirring for 30 min (process repeated four times) to yield a gel (1.70 g, 40% yield). The structure of the purified product was characterized by $^1\text{H NMR}$ (400 MHz, CDCl_3): δ 4.12 [br, 2H, $-(\text{C}=\text{O})\text{O}-\text{CH}_2-\text{CH}_2-$], 3.81–3.39 [m, 34H, $-\text{O}-\text{CH}_2-\text{CH}_2-\text{O}-$], 3.34 (s, 3H, $-\text{O}-\text{CH}_3$), 2.10 [br, 1H, $-\text{CH}_2\text{CH}(\text{C}=\text{O})-$], 2.02–1.36 [m, 2H, $-\text{CH}_2\text{CH}(\text{C}=\text{O})-$]. The resulting polymer was characterized by GPC using the method as described above: $M_n = 33,800$; $\text{PDI} = 1.52$.

Synthesis of PDMAEA₂₄–PEGMEA₄₀₀ (Random Copolymer). PEGMEA (3.46 g, 7.2 mmol) was added to a solution containing DMAEA (61.8 mg, 0.43 mmol), ACPA (0.5 mg, 0.0018 mmol), and CPADB (1.3 mg, 0.0045 mmol) in 2 mL of anisole. The mixture was deoxygenated by five freeze–vacuum–thaw cycles before it was heated up to 70 °C with stirring for 48 h. The reaction was then quenched by liquid nitrogen freezing, and the polymer gel was precipitated by addition of 20 mL of hexane and vigorously stirred for 30 min. After decanting the solvent, the residue was redissolved in 5 mL of dichloromethane and precipitated by the addition of 20 mL of hexane and vigorously stirred for 30 min (process repeated four times) to yield a gel (865 mg, 25% yield); $^1\text{H NMR}$ (400 MHz, CDCl_3): δ 4.12 [br, 2H, $-(\text{C}=\text{O})\text{O}-\text{CH}_2-\text{CH}_2-$], 3.75–3.44 (m, 34H, $-\text{O}-\text{CH}_2-\text{CH}_2-\text{O}-$), 3.35 (s, 3H, $-\text{O}-\text{CH}_3$), 2.26 [br, $\sim 1\text{H}$, $-\text{CH}_2\text{CH}(\text{C}=\text{O})-$], $-\text{N}(\text{CH}_3)_2$], 1.93–1.36 [m, 2H, $-\text{CH}_2\text{CH}(\text{C}=\text{O})-$], 5.30 (s, residue dichloromethane). The resulting polymer was characterized with GPC using the method described above: $M_n = 32,700$; $\text{PDI} = 1.94$.

Synthesis of qPDMAEA₂₄–PEGMEA₄₀₀ (Random Copolymer). Ethyl bromide (0.5 mL, 6.7 mmol) was added dropwise into a solution containing PDMAEA₂₄–PEGMEA₄₀₀ (random copolymer) (1.47 g) in 5 mL of acetone at 0 °C. The

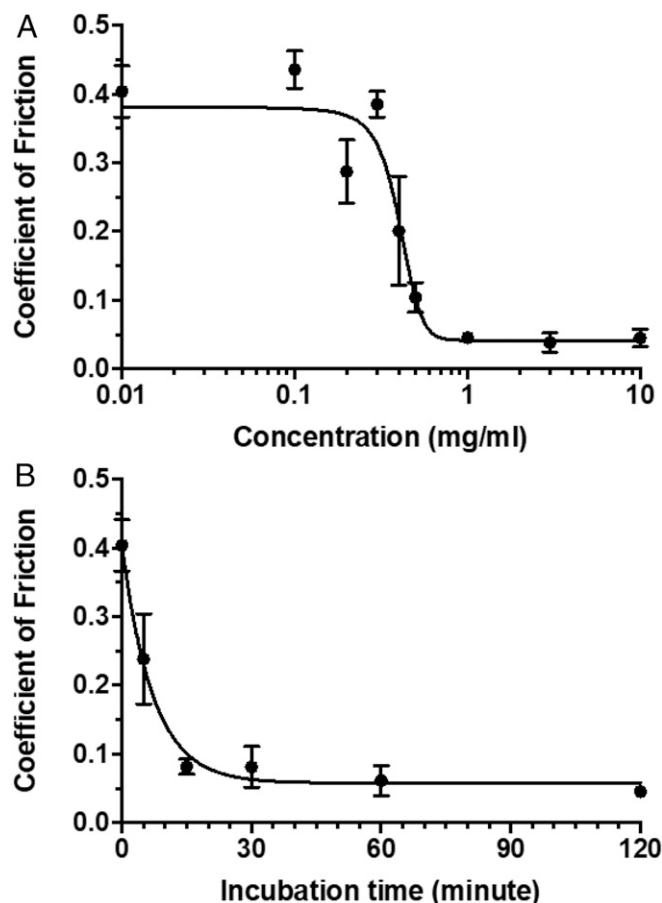


Fig. 6. Dose–response (A) and binding kinetics (B) curves of diblock copolymer ($n = 4-6$).

mixture was stirred for 48 h at room temperature and was then concentrated by evaporating most of the solvent with a dry nitrogen flow. The residue was dissolved in 3 mL of dichloromethane and precipitated with addition of 15 mL of hexane and vigorously stirred for 30 min (process repeated five times). The purified product was then dissolved in DI water and further purified by dialysis using Spectra/Por regenerated cellulose dialysis tubing (2 kDa MWCO) against DI water for an additional 48 h before lyophilization to yield a gel (1.36 g, 93%); ^1H NMR (400 MHz, D_2O) δ 4.08 [br, ~2H, $-(\text{C}=\text{O})\text{O}-\text{CH}_2-\text{CH}_2-$], 3.75–3.44 (m, 34H, $-\text{O}-\text{CH}_2-\text{CH}_2-\text{O}-$), 3.21 (s, 3H, $-\text{O}-\text{CH}_3$), 3.02 (s, ~0.2H, $-\text{N}^+(\text{CH}_3)_2\text{CH}_2\text{CH}_3$), 2.21 [br, 1H, $-\text{CH}_2\text{CH}(\text{C}=\text{O})-$], 2.02–1.44 [m, 2H, $-\text{CH}_2\text{CH}(\text{C}=\text{O})-$], 1.25 [br, ~0.1H, $-\text{N}^+(\text{CH}_3)_2\text{CH}_2\text{CH}_3$]. The resulting polymer was characterized with GPC using the method described above: $M_n = 33,400$; PDI = 1.71.

General Procedure for Tribological Testing. Friction coefficients were measured on our custom-built tribometer (18). Cartilage samples were obtained from the patellofemoral groove of neonatal (1 to 3 d old) bovine stifles. Shaped into a cartilage disk (6 mm in diameter by 2 mm high) by biopsy punch, samples were incubated in 1.5 M NaCl solution for 30 min, in PBS for an additional 60 min, and then in polymer solution (in PBS) for 0 to 120 min. The cartilage samples were loaded onto the tribometer against a polished glass flat counterface in a PBS bath with a tilt pad configuration (18). Before a friction test, samples were compressed to 30% strain and depressurized to an average normal load of 3.4 N within 60 min. After the fluid pressure reached equilibrium, the glass counterface was reciprocated at a linear oscillation speed of 0.3 mm/s. Both the normal load and friction force were measured by a biaxial load cell. Coefficients were calculated as an average ratio of friction force to normal load during the sliding and averaged for both the forward and reverse sliding directions. One-way ANOVA and Student's *t* test were used to determine the statistical difference.

SFA Experiment, Materials. Mica was purchased from S&J Trading Inc. as optical grade. PBS was purchased from Sigma-Aldrich.

SFA Experiment, Sample Preparation. Thin, homogeneous pieces of freshly cleaved, silvered mica were glued silver-side-down onto semicylindrical fused

silica discs ($R = 1$ cm and $R = 2$ cm) with UV curing glue (Norland 61). The surfaces were mounted opposing each other in a cross-cylindrical configuration in the SFA. After mounting, 50 μL of 3 mg/mL polymer solution in PBS was injected between the surfaces and incubated for 1 h. The surfaces were then rinsed in PBS, and a droplet of PBS was injected, leaving only a surface-bound layer of polymer for friction and film thickness measurements.

SFA Experiment, Friction Force Measurement. Once samples were prepared in the SFA, both normal and friction force measurements were performed. For normal force measurements, the lower surface was mounted on a double-cantilever spring ($k = 1,650$ N/m and $k = 185$ N/m) for normal force detection. For friction force measurements, the lower spring was mounted on a double-cantilever spring ($k = 1,650$ N/m) attached to a piezoelectric bimorph slider. The bimorph slider was sheared across the upper surface, which was mounted on a semiconductor strain gauge at 30 $\mu\text{m/s}$ to detect friction. Friction measurements were measured under incrementally increasing loads and friction coefficients were calculated using the slope of the friction vs. load data, $\Delta F_{\text{friction}}/\Delta F_{\text{Load}}$.

SFA Experiment, Film Thickness Measurement. Once samples were prepared in the SFA, the surfaces were brought together using a stepper motor at speeds <10 nm/s. The interference pattern, known as fringes of equal chromatic order, was recorded and analyzed to determine both the uncompressed film thickness (the film thickness where surface interaction is initially detected) and the compressed film thickness.

ACKNOWLEDGMENTS. This research was supported by National Institutes of Health Award R01 AR066667-01 (to D.P. and L.J.B.) and NSF Award DMR-1352299 (to D.G.). E.F. is grateful for the financial support of an NSF graduate research fellowship. This work was made possible by the Cornell Chemistry NMR facility and NSF-MRI (Grant CHE-1531632-PI: Aye) for NMR instrumentation support at Cornell University. This work made use of the Cornell Center for Materials Research Shared Facilities, which are supported through the NSF MRSEC program (DMR-1719875). We thank Dr. Ivan Keresztes for his expertise.

- G. A. Ateshian, The role of interstitial fluid pressurization in articular cartilage lubrication. *J. Biomech.* **42**, 1163–1176 (2009).
- S. S. Perry *et al.*, Tribological properties of poly(L-lysine)-graft-poly(ethylene glycol) films: Influence of polymer architecture and adsorbed conformation. *ACS Appl. Mater. Interfaces* **1**, 1224–1230 (2009).
- M. Müller, S. Lee, H. A. Spikes, N. D. Spencer, The influence of molecular architecture on the macroscopic lubrication properties of the brush-like co-polyelectrolyte poly(L-lysine)-g-poly(ethylene glycol) (PLL-g-PEG) adsorbed on oxide surfaces. *Tribol. Lett.* **15**, 395–405 (2003).
- T. Pettersson, A. Naderi, R. Makuška, P. M. Claesson, Lubrication properties of bottle-brush polyelectrolytes: An AFM study on the effect of side chain and charge density. *Langmuir* **24**, 3336–3347 (2008).
- X. Banquy, J. Burdyńska, D. W. Lee, K. Matyjaszewski, J. Israelachvili, Bioinspired bottle-brush polymer exhibits low friction and Amontons-like behavior. *J. Am. Chem. Soc.* **136**, 6199–6202 (2014).
- U. Raviv *et al.*, Lubrication by charged polymers. *Nature* **425**, 163–165 (2003).
- M. Wathier *et al.*, A large-molecular-weight polyanion, synthesized via ring-opening metathesis polymerization, as a lubricant for human articular cartilage. *J. Am. Chem. Soc.* **135**, 4930–4933 (2013).
- E. B. Zhulina, M. Rubinstein, Lubrication by polyelectrolyte brushes. *Macromolecules* **47**, 5825–5838 (2014).
- A. Lawrence *et al.*, Synthesis and characterization of a lubricin mimic (mLub) to reduce friction and adhesion on the articular cartilage surface. *Biomaterials* **73**, 42–50 (2015).
- D. A. Swann, H. S. Slayter, F. H. Silver, The molecular structure of lubricating glycoprotein-1, the boundary lubricant for articular cartilage. *J. Biol. Chem.* **256**, 5921–5925 (1981).
- G. D. Jay, K. A. Waller, The biology of lubricin: Near frictionless joint motion. *Matrix Biol.* **39**, 17–24 (2014).
- J. P. Gleghorn, A. R. C. Jones, C. R. Flannery, L. J. Bonassar, Boundary mode lubrication of articular cartilage by recombinant human lubricin. *J. Orthop. Res.* **27**, 771–777 (2009).
- G. D. Jay *et al.*, Prevention of cartilage degeneration and restoration of chondroprotection by lubricin tribosupplementation in the rat following anterior cruciate ligament transection. *Arthritis Rheum.* **62**, 2382–2391 (2010).
- A. A. Young *et al.*, Proteoglycan 4 downregulation in a sheep meniscectomy model of early osteoarthritis. *Arthritis Res. Ther.* **8**, R41 (2006).
- B. Zappone, G. W. Greene, E. Oroudjev, G. D. Jay, J. N. Israelachvili, Molecular aspects of boundary lubrication by human lubricin: Effect of disulfide bonds and enzymatic digestion. *Langmuir* **24**, 1495–1508 (2008).
- G. D. Jay, D. A. Harris, C. J. Cha, Boundary lubrication by lubricin is mediated by O-linked $\beta(1-3)$ Gal-GalNAc oligosaccharides. *Glycoconj. J.* **18**, 807–815 (2001).
- J. M. Pelet, D. Putnam, An in-depth analysis of polymer-analogous conjugation using DMTMM. *Bioconjug. Chem.* **22**, 329–337 (2011).
- J. P. Gleghorn, L. J. Bonassar, Lubrication mode analysis of articular cartilage using stripebeck surfaces. *J. Biomech.* **41**, 1910–1918 (2008).
- A. R. C. Jones *et al.*, Binding and localization of recombinant lubricin to articular cartilage surfaces. *J. Orthop. Res.* **25**, 283–292 (2007).
- R. C. Andresen Eguiluz *et al.*, Synergistic interactions of a synthetic lubricin-mimetic with fibronectin for enhanced wear protection. *Front. Bioeng. Biotechnol.* **5**, 36 (2017).
- M. Daniel, Boundary cartilage lubrication: Review of current concepts. *Wien Med. Wochenschr.* **164**, 88–94 (2014).
- S. N. Ramakrishna, R. M. Espinosa-Marzal, V. V. Naik, P. C. Nalam, N. D. Spencer, Adhesion and friction properties of polymer brushes on rough surfaces: A gradient approach. *Langmuir* **29**, 15251–15259 (2013).
- C. Perrino, S. Lee, S. W. Choi, A. Maruyama, N. D. Spencer, A biomimetic alternative to poly(ethylene glycol) as an antifouling coating: Resistance to nonspecific protein adsorption of poly(L-lysine)-graft-dextran. *Langmuir* **24**, 8850–8856 (2008).
- K. J. Samaroo, M. Tan, D. Putnam, L. J. Bonassar, Binding and lubrication of biomimetic boundary lubricants on articular cartilage. *J. Orthop. Res.* **35**, 548–557 (2017).
- A. Singh *et al.*, Enhanced lubrication on tissue and biomaterial surfaces through peptide-mediated binding of hyaluronic acid. *Nat. Mater.* **13**, 988–995 (2014).
- G. Morgese, E. Cavalli, J. G. Rosenboom, M. Zenobi-Wong, E. M. Benetti, Cyclic polymer grafts that lubricate and protect damaged cartilage. *Angew. Chem. Int. Ed. Engl.* **57**, 1621–1626 (2018).